

## Supplementary Information

For

### Hierarchically Multifunctional TiO<sub>2</sub> Nano-thorn Membrane for Water Purification

Hongwei Bai, Zhaoyang Liu\*, and Darren Delai, Sun\*

*School of Civil & Environmental Engineering, Nanyang Technological University, Singapore  
639798*

[zyliu@ntu.edu.sg](mailto:zyliu@ntu.edu.sg); [ddsun@ntu.edu.sg](mailto:ddsun@ntu.edu.sg)

#### Experimental section

##### Hydrothermally Synthesis of TiO<sub>2</sub> Nano-thorn Sphere

All chemical reagents were purchased from Aldrich unless otherwise stated. 2.5 mL TiCl<sub>3</sub> (MERCK, with 20 % HCl content) was readily dissolved in 27.5 mL saturated NaCl solution. The pH value of the mixed solution was adjusted to 3 with NaOH, then the mixture was filled into a 40 mL Teflon-lined stainless steel autoclave. The autoclave was capped tightly, put inside an electrical oven and heated to 190 °C for 3h.

The autoclave was naturally cooled down in air, and was opened gently with a pungent smell emitting. Then poured off the clear supernatant carefully, and transferred the white sediments, which were the synthesized TiO<sub>2</sub> nano-thorn spheres into a clean centrifugation tube. Washed the TiO<sub>2</sub> nano-thorn spheres sufficiently with deionized (DI) water and dried it for further characterization.

##### Assembly of Hierarchical TiO<sub>2</sub> Nano-thorn Membrane

100 mg successfully synthesized TiO<sub>2</sub> nano-thorn spheres were uniformly deposited on one piece of commercial cellulose acetate membrane (Millipore membrane discs Ø 47 mm, 0.20

$\mu\text{m}$ ), which was properly located at the bottom of filtration cup (Figure S7a). Then the filtration cup was filled with DI water and slowly opened the  $\text{N}_2$  gas valve to provide pressure, as a result of the combined action of water and regularly discharged  $\text{N}_2$  gas, the  $\text{TiO}_2$  nano-thorn spheres were uniformly assembled on the cellulose acetate membrane and were compressed to form a hierarchically structured  $\text{TiO}_2$  nano-thorn membrane. This membrane was assembled and characterized successfully. It was used to do further application test to evaluate its flux performance and photocatalytic oxidation activities.

As a comparison, using the above mentioned method, 100 mg  $\text{TiO}_2$  P25 was also deposited on another piece of commercial cellulose acetate membrane to form a  $\text{TiO}_2$  P25 deposited cake layer to simulate the assembled  $\text{TiO}_2$  nano-thorn membrane, which was characterized and used for further application test such as flux performance investigation.

## Characterization

The structure and crystal phase of  $\text{TiO}_2$  nano-thorn spheres were examined using Shimadzu XRD-6000 X-ray diffractometer with monochromated high-intensity  $\text{Cu K}\alpha$  radiation ( $\lambda = 1.5418 \text{ \AA}$ ) operated at 40 kV and 30 mA. The scanning rate was  $2^\circ/\text{min}$ .

The morphologies of  $\text{TiO}_2$  nano-thorn spheres and the assembled  $\text{TiO}_2$  nano-thorn membrane were observed by field-emission scanning electron microscopy (FESEM, Jeol JSM-6340F) and transmission electron microscopy (TEM, Jeol JEM-2010). Energy dispersive x-ray (EDS) measurement was conducted using the EDAX system attached to the same field emission scanning electron microscopy with carbon tape and gold sputtering used for the sample preparations.

BET surface area and pore size distribution of  $\text{TiO}_2$  nano-thorn spheres were determined at liquid nitrogen temperature (77 K) using a Micromeritics ASAP 2040 system. Before the measurement, 0.1 g sample was out-gassed under vacuum for 10 h at  $250^\circ\text{C}$ .

## Concurrent Photocatalytic Oxidation and Membrane Filtration

After the hierarchical TiO<sub>2</sub> nano-thorn membrane was assembled. A dead-end apparatus, as shown in Figure S7b which has been reported by us previously<sup>1, 2</sup> was used for the investigation of concurrent photocatalytic oxidation and membrane filtration. In this concurrent processes, a specific UVP lamp (254 nm, 40 mW/cm<sup>2</sup>), equipped with a specific power source, was suspended above the assembled hierarchical TiO<sub>2</sub> nano-thorn membrane.

For the photodegradation of MB, 60 ml MB solution with an initial concentration of 50 mg/L was filled into the filtration cup. The MB solution in the filtration cup was kept in the dark for 1 hour to ensure the adsorption equilibrium had been reached and then turned on the UV light and the transmembrane pressure (TMP). The TMP was maintained around 0.05 MPa during the whole processes. 3 mL permeates were collected to measure the UV-adsorption value at 605 nm (the major adsorption peak of herein used MB, is around 605)<sup>3, 4</sup> at 10 min, 20 min, and 30 min. As a contrast, the photodegradation of MB by TiO<sub>2</sub> P25 deposited membrane was also conducted simultaneously.

For the photodegradation of humic acid (HA), 60 ml HA solution with an initial concentration of 30 mg/L was filled into the filtration cup. The filtration cup with HA solution was kept in the dark for 2 hour to ensure the adsorption equilibrium had been reached and then turned on the UV light and the transmembrane pressure (TMP). TMP was maintained around 0.05 MPa during the whole processes. 3 mL permeates were collected to measure the UV-adsorption value at 436 nm at 20 min, 40 min, and 60 min. As a contrast, the photodegradation of HA by TiO<sub>2</sub> P25 deposited membrane was also conducted simultaneously.

The photocatalytic degradation of MB/HA as a function of the irradiation time in the presence of hierarchical TiO<sub>2</sub> nano-thorn membrane or TiO<sub>2</sub> P25 deposited membrane was observed to follow first-order kinetic reaction. Thus, the photocatalytic reaction can simply be described by:

$$r = -d[c]/dt = k [c] \quad (1)$$

or

$$-\ln [c]/c_0 = kt \quad (2)$$

Where  $r$  is the degradation rate of MB or HA,  $[c]$  is the concentration of MB or HA,  $c_0$  is initial concentration of MB or HA,  $t$  is the irradiation time, and  $k$  is the first order kinetic reaction rate constant.<sup>1,2</sup>

## Membrane Flux Performance Investigation

Besides the investigation of photocatalytic activity, the flux performance of hierarchical TiO<sub>2</sub> nano-thorn membrane and TiO<sub>2</sub> P25 deposited membrane over TMP was also investigated in the same dead-end apparatus as shown in Figure S7a without the UV light irradiation. This bench-scale system comprise of a membrane cell with a filtration cup volume of 60 mL, which housed the TiO<sub>2</sub> nano-thorn membrane. The effective membrane area was 13.4 cm<sup>2</sup>. Pressure was provided by a compressed N<sub>2</sub> gas cylinder that was connected to the filtration cup. Permeate was collected and its mass was measured continuously over time using a weighing balance connected to a data logger. Data were collected on a per second basis and averaged per minute. Permeate flux was calculated on the basis of permeate mass divided by effective surface area and filtration time, unit is L/(m<sup>2</sup>.min). For the evaluation of membrane flux performance, at the steady state under a given TMP, average permeate flux was measured. As a contrast, using the same method, the membrane flux of TiO<sub>2</sub> P25 deposited membrane was also evaluated and the corresponding permeate flux at different TMP was calculated and recorded. Finally, the relationship between permeate flux and TMP for hierarchical TiO<sub>2</sub> nano-thorn membrane and P25 deposited membrane were drawn and displayed in Figure 3c.

**References:**

1. Xiwang Zhang, Jia Hong Pan, Alan Jiahong Du, Weijiong Fu, Darren D. Sun, and James O. Leckie, *Water Research* **2009**, *43*, 1179-1186.
2. Xiwang Zhang, Alan Jianhong Du, Peifung Lee, Darren Delai Sun, and James O. Leckie, *Appl. Catal. B: Environ.* **2008**, *84*, 262-267.
3. Emory Braswell, *J. Phys. Chem.* **1968**, *72* (7), 2477–2483
4. Andrew Mills, Mubeen Sheik, Christopher O' Rourke, Michael McFarlane, *Appl. Catal. B: Environ.* **2009**, *89*, 189-195.

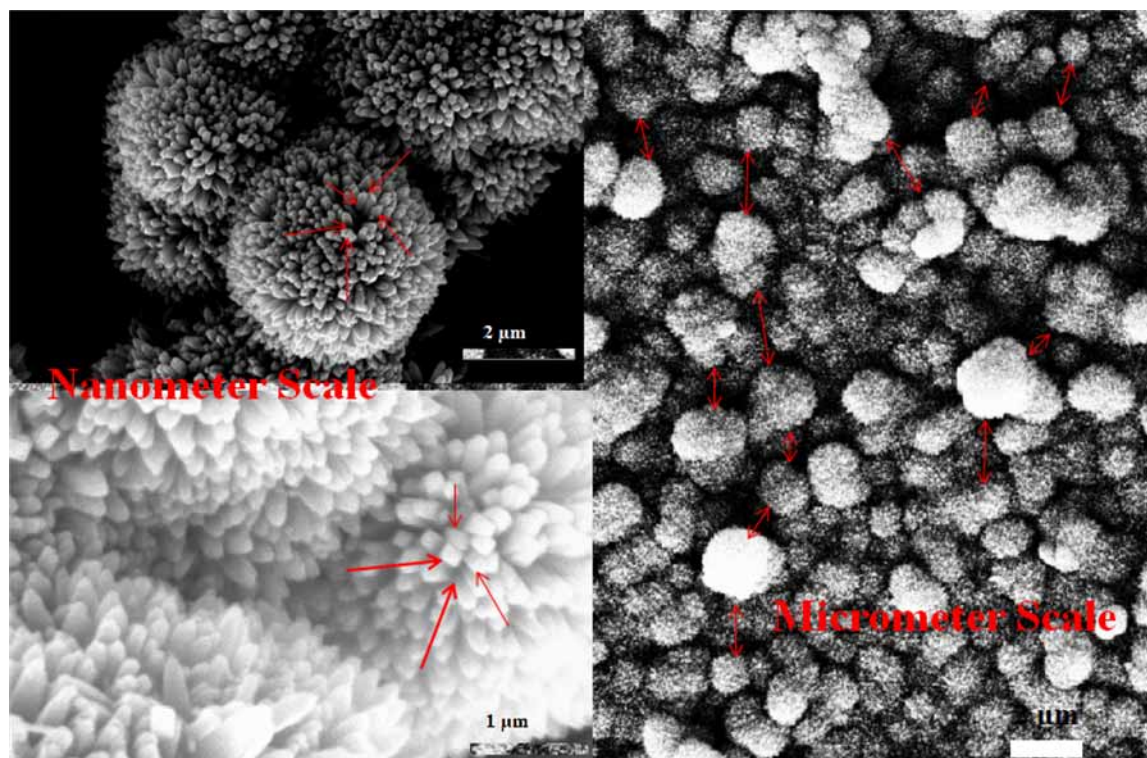


**Figure S1.** SEM images of TiO<sub>2</sub> nano-thorn membrane with a clear indication of the multi-scale hierarchical structure. Wherein, the nano-scale is referred to the distances between different TiO<sub>2</sub> nano-thorns, the micro-scale is referred to the distances between different spheres

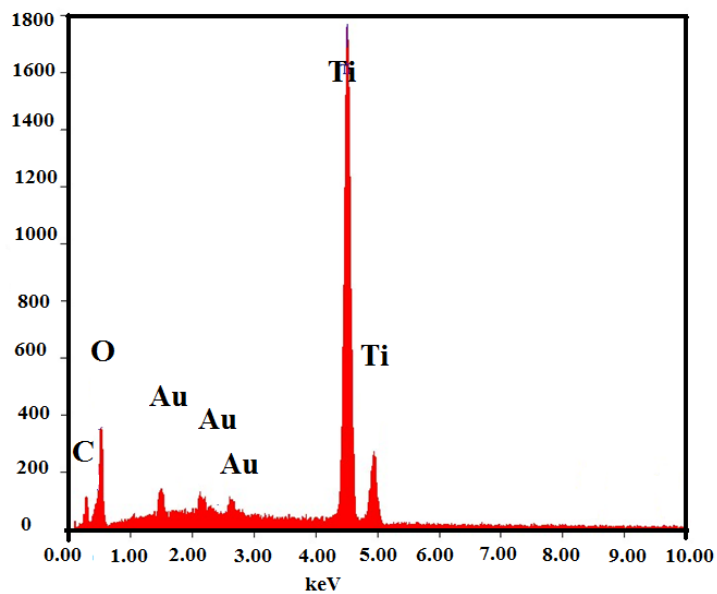


**Figure S2.** EDS spectra of TiO<sub>2</sub> nano-thorn membrane

**Table S1.** Element contents of TiO<sub>2</sub> nano-thorn membrane corresponding to EDS spectra

Element	keV	Mass %	Atom %
C K	0.277	2.42	1.4198
O K	0.525	25.44	10.0081
Ti K	4.508	69.71	86.2975
Au K	2.121	2.43	2.2746
Total		100	100

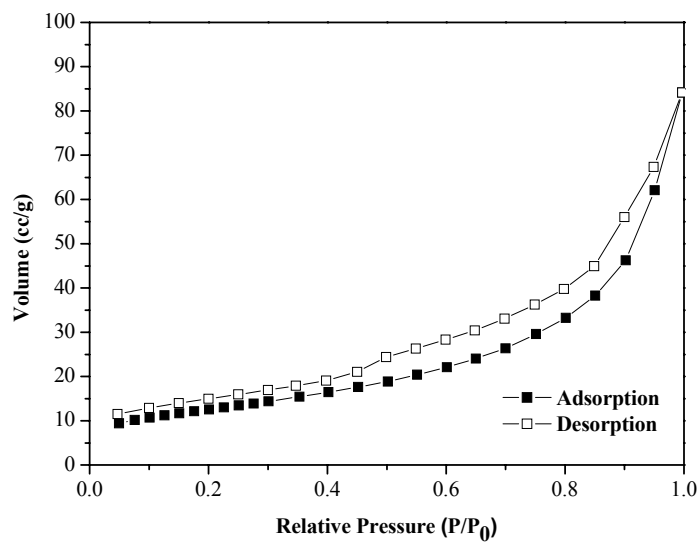


**Figure S3.** N<sub>2</sub> adsorption/desorption isotherm curve of TiO<sub>2</sub> nano-thorn spheres assembled on polymer membrane



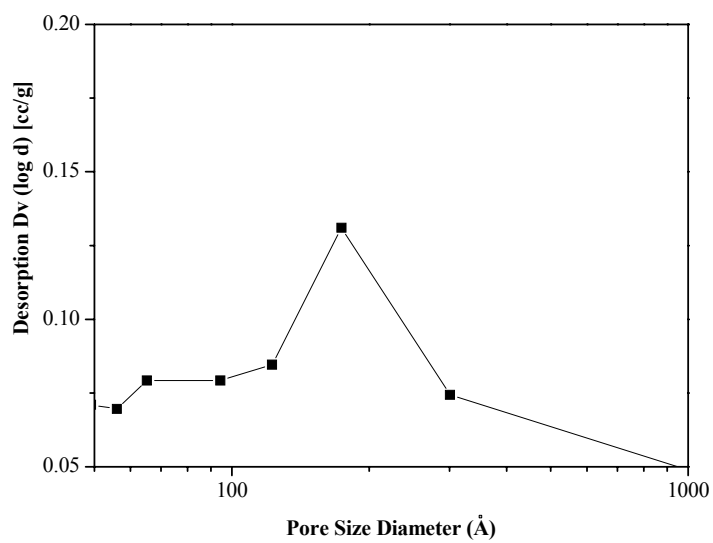


**Figure S4.** Pore size distribution of TiO<sub>2</sub> nano-thorn spheres assembled on polymer membrane determined by N<sub>2</sub> adsorption

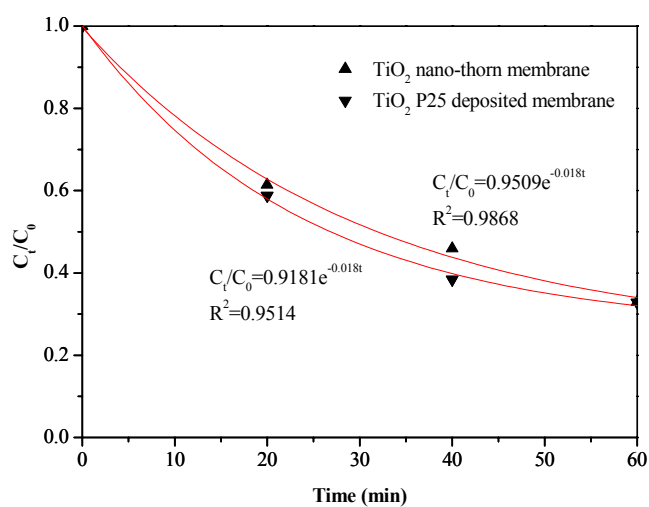


**Figure S5.** The first order kinetic curve of photodegradation of HA by TiO<sub>2</sub> nano-thorn membrane and TiO<sub>2</sub> P25 deposited membrane

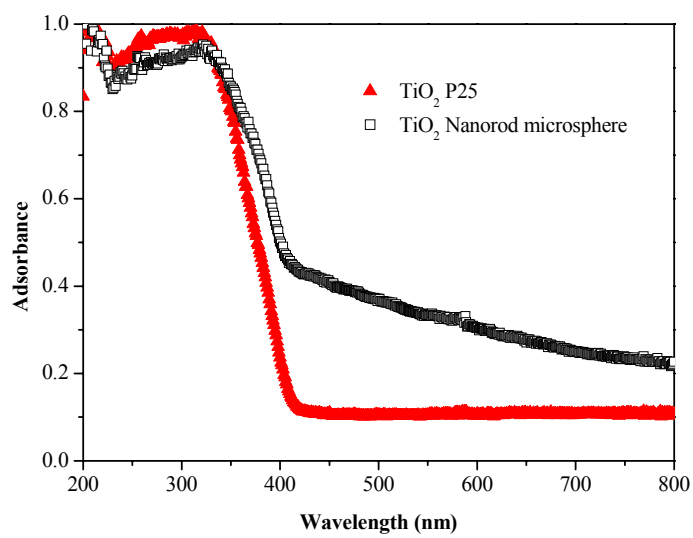


**Figure S6.** UV-Visible spectra of TiO<sub>2</sub> nano-thorn spheres assembled on polymer membrane and TiO<sub>2</sub> P25 deposited membrane

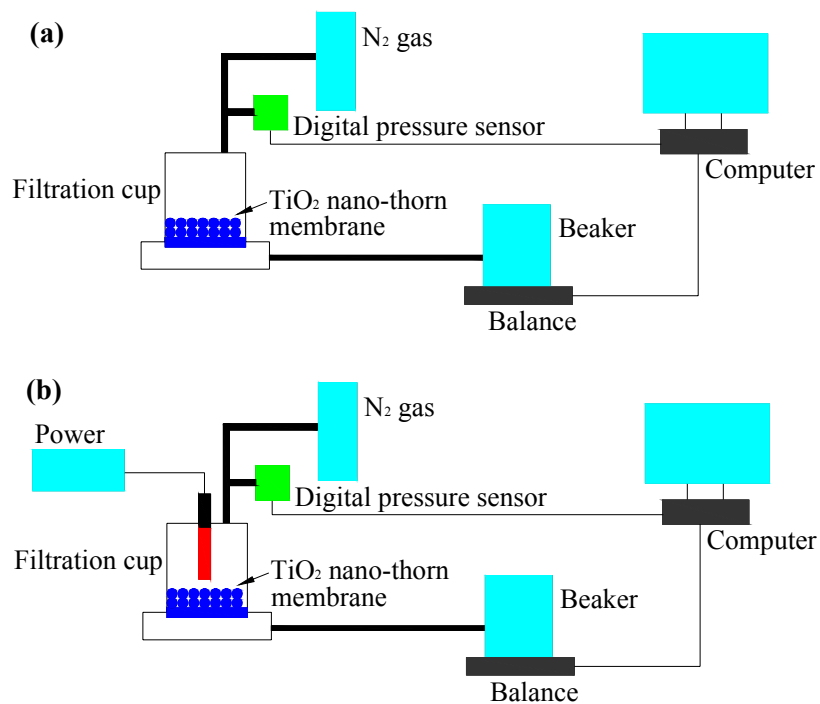


**Figure S7.** (a) The apparatus scheme of flux performance investigation, and (b) apparatus scheme of concurrent photocatalytic oxidation and membrane filtration

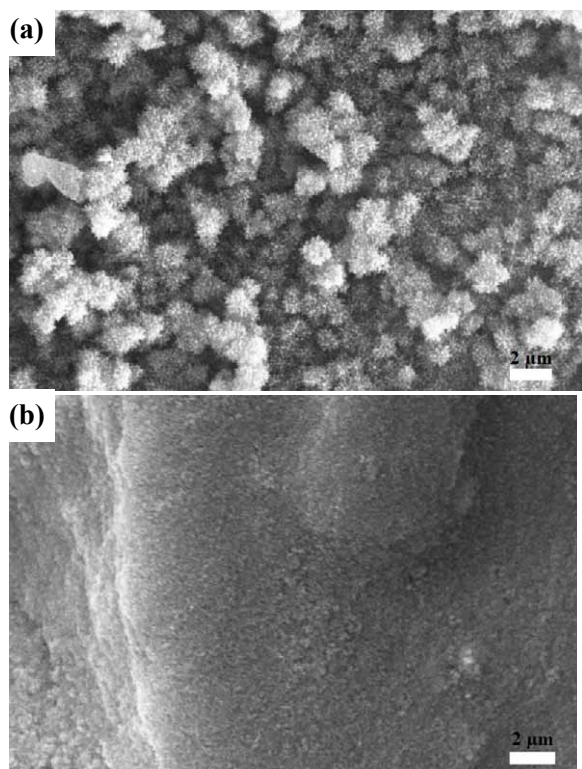


**Figure S8.** SEM images of (a) hierarchical TiO<sub>2</sub> nano-thorn membrane surface and (c) P25 deposited membrane after filtration

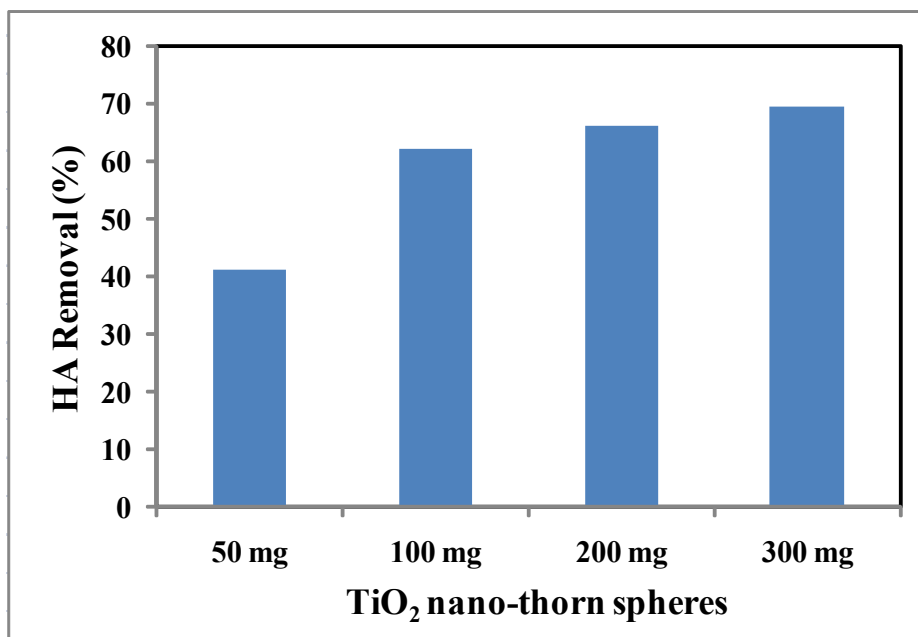


**Figure S9.** Effect of membrane thickness on the photocatalytic performance of hierarchical TiO<sub>2</sub> nano-thorn membrane

Explanation:

Through controlling the amount of the TiO<sub>2</sub> nano-thorn spheres deposited on the polymer membrane (Cellulose acetate, Millipore, USA) surface, the thickness of the TiO<sub>2</sub> nano-thorn membrane can be well adjusted. Here, four pieces of TiO<sub>2</sub> nano-thorn membranes with different amounts of TiO<sub>2</sub> nano-thorn spheres on the polymer membrane surfaces were assembled. The photocatalytic performances (HA removal, %) as the function of the thickness of these membranes were investigated as shown in Figure S9. And the experimental results demonstrated that the photocatalytic performances were affected significantly when the deposited TiO<sub>2</sub> nano-thorn spheres is below 100 mg, and under this situation, more TiO<sub>2</sub> nano-thorn spheres means more photocatalysts involved in the reaction. But when the deposited TiO<sub>2</sub> nano-thorn spheres exceed 200 mg, the increase of photocatalytic performance has little difference with the increased thickness; this is due to that photocatalysts need light to activate them and the underneath of the thick TiO<sub>2</sub> membrane can't get light, therefore can't taking part in the photocatalytic reaction. In our research, we choose 100 mg as the appropriate amount of photocatalysts.

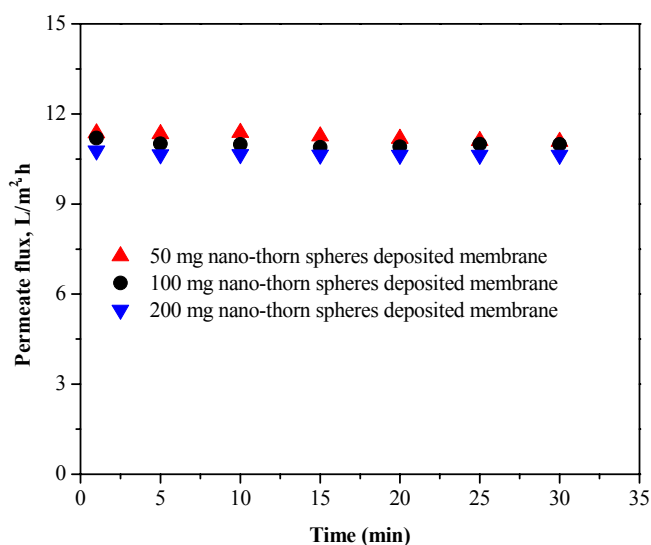


**Figure S10.** Effect of membrane thickness on the filtration performance of TiO<sub>2</sub> nano-thorn membrane

Explanation:

Through controlling the amount of TiO<sub>2</sub> nano-thorn spheres deposited on the polymer membrane (Cellulose acetate, Millipore, USA) surface, the thickness of the TiO<sub>2</sub> nano-thorn membranes can be well adjusted. Here, three pieces of hierarchical TiO<sub>2</sub> nano-thorn membranes with different amounts of TiO<sub>2</sub> nano-thorn spheres on the polymer surfaces were assembled, the thickness of these membranes are varied according to the amount of deposited TiO<sub>2</sub> nano-thorn spheres. The filtration performances were investigated in the lab-scale dead end setup as Figure S7a, with transmembrane pressure of 2 Bar and DI water as feed water. The experimental results demonstrated that three membranes of different thickness showed the identical flux around 11 L/(m<sup>2</sup>.h). This indicated that the thickness of the TiO<sub>2</sub> nano-thorn membranes has little affection on the filtration performance because of the hierarchical structures of these TiO<sub>2</sub> nano-thorn spheres, which is easy for water pass through.

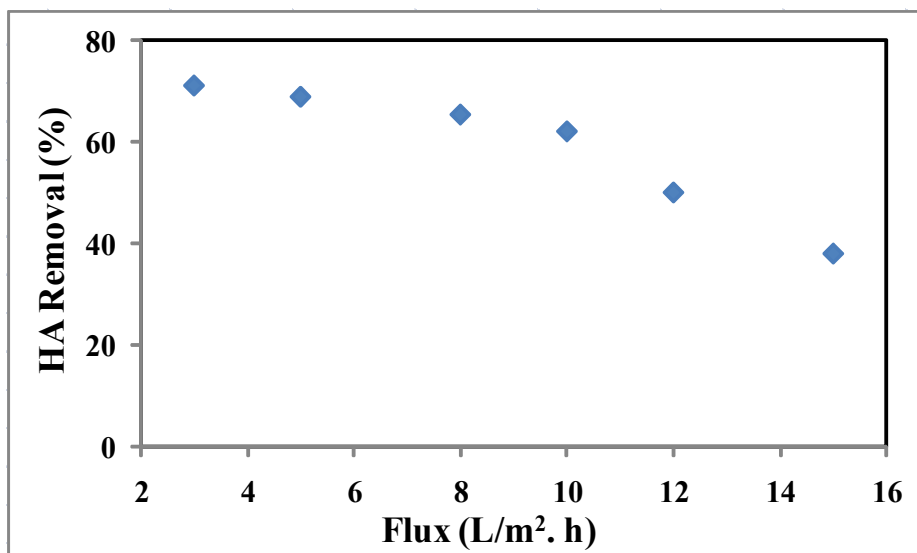


**Figure S11.** Effect of the permeate flux on anti-fouling capacity of TiO<sub>2</sub> nano-thorn membrane

Explanation:

The above experimental conditions are: 100 mg TiO<sub>2</sub> nano-thorn spheres were deposited on one piece of polymer membrane; the concentration of HA feed water was 30 mg/L; and the photocatalytic reaction time was 30 min. The HA removal rate was measured under different permeate flux. The experimental results demonstrated that HA removal rate generally decreased with the increase of permeate flux; but when the permeate flux was less than 10 L/(m<sup>2</sup>.h), the decrease of HA removal rate was not significant, which means that the flux of 10 L/(m<sup>2</sup>.h) is the balance point between photocatalytic degradation of HA and flux under our experimental condition. When the permeate flux was larger than 10 L/(m<sup>2</sup>.h), a significant decrease of HA removal rate started, which means longer reaction time is needed to reach the same photo-degradation effect at a given permeate flux condition.